

Controlling Acetylene Adsorption and Reactions on Pt–Sn Catalytic Surfaces

Jie Gao,[†] Haibo Zhao,[§] Xiaofang Yang,^{§§} Bruce E. Koel,^{‡,*} and Simon G. Podkolzin^{†,*}

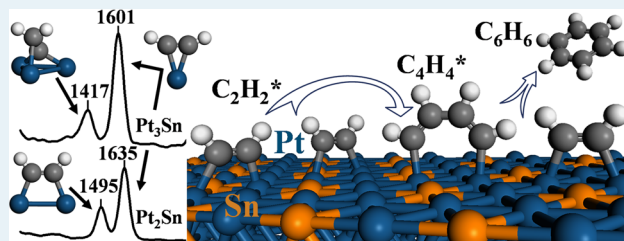
[†]Department of Chemical Engineering and Materials Science, Stevens Institute of Technology, Hoboken, New Jersey 07030, United States

[‡]Department of Chemical and Biological Engineering, Princeton University, Princeton, New Jersey 08544, United States

Supporting Information

ABSTRACT: Acetylene reactivity as a function of Sn concentration on Pt catalytic surfaces was studied by comparing adsorption and reactions of regular and deuterated acetylene at 90–1000 K on three surfaces, Pt(111), Pt₃Sn/Pt(111), and Pt₂Sn/Pt(111), using high-resolution electron energy loss spectroscopy, temperature-programmed desorption, and density functional theory calculations. The strongly adsorbed di- σ / π -bonded acetylene species, which dominate on pure Pt, were not detected on the Pt–Sn surfaces. The presence of Sn is also shown to suppress acetylene decomposition and, as a result, to maintain adsorbed acetylene in the molecular form as weakly adsorbed π - and di- σ -bonded species. The destabilization of adsorbed acetylene makes associative reactions with the formation of dimers (C₄ hydrocarbons) and trimers (benzene) progressively more energetically favorable with increasing Sn concentration. Acetylene adsorption modes and reactions on Pt catalytic surfaces can, therefore, be controlled with Sn alloying. The concentration of Sn needs to be an optimal level for catalytic activity since all hydrocarbon species bind preferentially only to Pt sites.

KEYWORDS: ethyne, adsorption, platinum, platinum–tin alloy, cyclotrimerization, HREELS, TPD, DFT



Tin is a common promoter in platinum-based catalyst formulations. Pt–Sn bimetallic catalysts are used in diverse commercial applications, ranging from reforming of gasoline for improving its octane number to hydrocarbon hydrogenation, dehydrogenation, isomerization, and oxidation in petroleum refining and chemical industries. There is also a renewed research interest in properties of Pt–Sn catalysts because of promising new applications in fuel cells and production of alternative renewable transportation fuels based on biomass conversion. For example, Pt-based catalysts and bimetallics with Sn were found to be catalytically active for aqueous-phase reforming of biomass feedstocks for the production of high purity hydrogen for fuel cells and generation of synthesis gas for subsequent conversion to synthetic transportation fuels or chemical feedstocks.¹ The effect of Sn on properties of Pt catalysts, however, is not well understood at the molecular level.

Our previous studies showed that the presence of Sn opens a new catalytic pathway for acetylene on Pt surfaces: while acetylene only decomposes upon heating on the Pt(111) surface, it forms dimers (C₄ hydrocarbons) and trimers (benzene) on Pt–Sn catalysts.² The amount of produced C₄ and C₆ products was found to be larger with increased Sn concentration. In another study, the catalytic activity of the Pt₂Sn surface alloy for acetylene dimerization and trimerization in the presence of gas-phase hydrogen was found to be 4–5 times higher than that over Pt(111).³ In this work, high-

resolution electron energy loss spectroscopic (HREELS) and temperature-programmed desorption (TPD) measurements are combined with density functional theory (DFT) calculations for identification of acetylene adsorption modes and understanding at the molecular level the effect of Sn alloying on acetylene reactivity on well-defined active sites of single crystals.

Two Pt–Sn alloys were prepared by evaporating Sn onto a Pt(111) single crystal surface and subsequently annealing the samples to 1000 K. This high annealing temperature ensured that the generated surfaces were stable (no surface reconstruction) under all subsequent testing conditions. Depending on the initial amount of Sn, the annealed surface exhibited either a (2 × 2) or (√3 × √3)R30° pattern in low-energy electron diffraction (LEED) measurements. Sn was incorporated only in the top surface layer, forming, respectively, Pt₃Sn/Pt(111) and Pt₂Sn/Pt(111) surface alloys.⁴ The geometric arrangement of Sn atoms on the alloy with the higher concentration of Sn, the Pt₂Sn/Pt(111) surface, completely eliminated three-fold Pt surface sites (fcc and hcp sites). DFT models of Pt(111) and two Pt–Sn alloy surfaces are shown in Figure 1. These Pt surfaces are not approximations of catalytic active sites, but they are exactly the same surfaces that were used experimentally in this study.

Received: March 14, 2013

Revised: April 24, 2013

Published: April 26, 2013

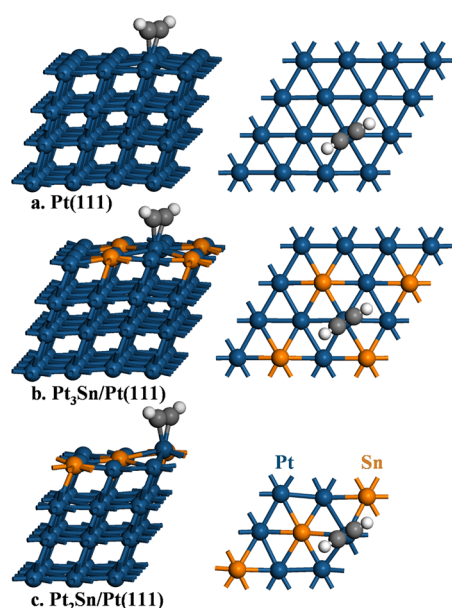


Figure 1. DFT models of Pt(111) and two Pt–Sn surface alloys with π -bonded acetylene. Left column shows full periodic unit cells used to construct an infinite surface. Right column shows the top view of only the first surface metal layer for clarity.

The effect of Sn alloying was evaluated with adsorption and reactivity measurements using regular (C_2H_2) and fully deuterated (C_2D_2) acetylene. Acetylene was initially adsorbed at 90 K. Acetylene adsorption and subsequent transformations of adsorbed hydrocarbon species upon heating to higher temperatures were monitored with TPD measurements at 90–1000 K and by collecting HREELS spectra at different temperatures at 90–500 K. The spectra were interpreted based on results of DFT calculations with vibrational analyses.

HREELS spectra for C_2H_2 and C_2D_2 on the two Pt–Sn alloy surfaces after heating to 200 K are shown in Figure 2. The spectrum for C_2D_2 on the Pt_2Sn surface in Figure 2b carbon–carbon bond stretching, ν_{CC} , peaks at 1451 and 1635 cm^{-1} . The same two bands were observed at the dosing temperature of 90 K. Since acetylene is expected to adsorb molecularly at this low temperature and there are only two types of Pt sites on the Pt_2Sn surface, these two peaks should be due to acetylene

adsorbed on bridge and atop Pt sites. The DFT calculated vibrational modes for C_2D_2 di- σ -bonded to a bridge Pt–Pt site ($\mu_2-\eta^2$ configuration, Figure 3c) at 1429 cm^{-1} and π -bonded to an atop Pt site (η^2 configuration, Figure 1c) at 1669 cm^{-1} (Table 1) are in good agreement with the experimental values

Table 1. DFT Calculations for the Carbon–Carbon Bond-Stretching Vibrational Mode, ν_{CC} , for Regular (and fully deuterated) C_2 Hydrocarbon Species Adsorbed on Different Surfaces, cm^{-1}

	Pt(111)	Pt ₃ Sn	Pt ₂ Sn
di- σ / π CH–CH	1351 (1321)	1326 (1295)	N/A
di- σ CH–CH	1426 (1385)	1460 (1419)	1476 (1429)
π CH–CH	1830 (1675)	1825 (1674)	1817 (1669)
C–CH ₂ ^a	1460 (1322)	1445 (1370)	1535 (1497)
C–CH ₂ ^b	1278 (1019)	1312 (997)	1343 (995)
C–CH	1379 (1345)	1552 (1503)	1790 (1716)

^aCoupled vibration δ_{CH_2}/ν_{CC} . ^bCoupled vibration ν_{CC}/δ_{CH_2} .

and, therefore, confirm this assignment. In the $\mu-\eta$ adsorbate notation, the μ index denotes the number of bridging metal surface atoms bonded to the adsorbed hydrocarbon, and the η index denotes the number of carbon atoms in the adsorbed hydrocarbon that are bonded to these surface metal atoms. On heating, the less strongly adsorbed π -bonded acetylene (peak at 1635 cm^{-1} in Figure 2b) desorbs preferentially, followed by more strongly adsorbed di- σ -bonded species (peak at 1451 cm^{-1}). Importantly, no new vibrational peaks in the ν_{CC} region for C_2 species are observed as acetylene desorbs (the main C_2D_2 TPD peak is observed at 386 K), confirming that acetylene desorption is mostly from molecules that have not undergone rearrangement or decomposition.

The two vibrational peaks for C_2D_2 adsorbed on the Pt_3Sn surface at 200 K are the same as those on the Pt_2Sn surface (Figure 2b). This similarity indicates that the acetylene adsorption modes are also the same: di- σ -bonded to a bridge Pt–Pt site and π -bonded to an atop Pt site, despite the availability of three-fold Pt adsorption sites on the Pt_3Sn surface. The presence of neighboring Sn atoms must be destabilizing acetylene adsorption on three-fold Pt sites, thus making bridge and atop Pt sites more preferable at high hydrocarbon surface coverage. The similarity of C_2D_2

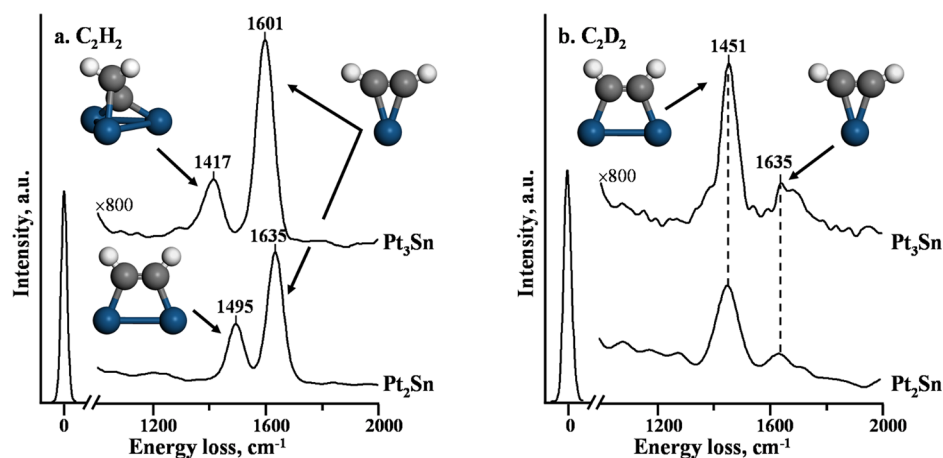


Figure 2. HREELS spectra of (a) C_2H_2 and (b) C_2D_2 on $Pt_3Sn/Pt(111)$ and $Pt_2Sn/Pt(111)$ surface alloys at 200 K with peak assignments to C_2 hydrocarbon species based on a comparison with DFT calculated normal vibrational modes in Table 1.

adsorption modes on the two alloy surfaces is further evidenced by the similarity in the position of the main C_2D_2 desorption peaks in TPD measurements: 380 K for the Pt_3Sn surface and 386 K for the Pt_2Sn surface.

Since C_2D_2 adsorbs only molecularly on the Pt_2Sn surface at 200 K (Figure 2b), the same molecular adsorption modes are expected for C_2H_2 at the same temperature (Figure 2a). The experimental peaks at 1495 and 1635 cm^{-1} for C_2H_2 at 200 K in Figure 2a can, therefore, be assigned to, correspondingly, ν_{CC} of di- σ -bonded species on a bridge Pt–Pt site and π -bonded species on an atop Pt site. The positions of ν_{CC} peaks for identical surface species for CH–CH should be at higher wavenumbers than those for CD–CD because of the lower atomic mass of H compared with that of D. The DFT calculations summarized in Table 1 correctly predict this shift and the position of ν_{CC} for the di- σ -bonded acetylene: the experimental wavenumbers are 1495 cm^{-1} for CH–CH and 1451 cm^{-1} for CD–CD, and the corresponding calculated vibrational modes are 1476 and 1429 cm^{-1} . The agreement between these calculated values, which are reported in Table 1 without any adjustments, and experimental peak positions for di- σ -bonded species is within ~ 30 cm^{-1} . Our previous calculations for vibrational modes of ethylene oxide and cyclohexanone adsorbed on the same Pt(111), Pt_3Sn , and Pt_2Sn surfaces were also in good agreement with HREELS peaks.⁵ The calculated vibrational mode for weakly bound π -bonded CH–CH species at 1817 cm^{-1} in Table 1 is, however, somewhat close to the value for gas-phase acetylene (1974 cm^{-1}) and significantly overestimates the observed experimental wavenumber of 1635 cm^{-1} in Figure 2a. This discrepancy can be attributed to the difficulty of a sufficiently accurate description of π -bonded species, in which small changes in the geometries of adsorbates from the gas-phase structure cause significant differences in vibrational wavenumbers.

The geometries and, correspondingly, vibrational wavenumbers for molecular CH–CH species on atop and bridge Pt sites for the two alloy surfaces should be similar. As a result, the experimental peak at 1601 cm^{-1} for C_2H_2 on the Pt_3Sn surface at 200 K (Figure 2a), which is at a position similar to the peak at 1635 cm^{-1} for Pt_2Sn at the same temperature, can be assigned to π -bonded acetylene on atop Pt sites (Figure 1b). The second peak at 1417 cm^{-1} for the Pt_3Sn surface in Figure 2a, however, is not consistent with the peak at 1495 cm^{-1} for di- σ -bonded acetylene on the Pt_2Sn surface. It is also not consistent with di- σ/π -bonded acetylene in a three-fold Pt site ($\mu_3-\eta^2$ configuration), which is the most stable acetylene configuration on Pt(111) and expected to remain in this configuration at high hydrocarbon coverage⁶ with a reported⁷ HREELS peak for ν_{CC} at ~ 1310 cm^{-1} (the corresponding calculated vibrational mode in Table 1 for the model in Figure 3a is 1351 cm^{-1}). Since microscopy and isotope spectroscopic studies of acetylene reactivity on Pt(111) suggest that the initial reaction is the intramolecular H transfer with the formation of C–CH₂ vinylidene species,⁸ the peak at 1417 cm^{-1} for the Pt_3Sn surface can be assigned to δ_{CH_2}/ν_{CC} (coupled vibrational mode with CH₂ scissoring, i.e., in plane symmetric bending, and C–C bond stretching) of C–CH₂ species. The calculated value for this mode of 1445 cm^{-1} for di- σ/π -bonded C–CH₂ ($\mu_3-\eta^2$ configuration) on three-fold Pt sites of the Pt_3Sn surface (Table 1) confirms this assignment. The second C–CH₂ vibrational mode, ν_{CC}/δ_{CH_2} (C–C bond stretching coupled with CH₂ scissoring) computationally predicted at

1312 cm^{-1} was not observed, likely due to its lower expected intensity. For comparison, the calculated values for these two vibrational modes of C–CH₂ on Pt(111) in Table 1 of 1460 cm^{-1} for δ_{CH_2}/ν_{CC} and 1278 cm^{-1} for ν_{CC}/δ_{CH_2} are in good agreement with a recent computational study (1413 and 1256 cm^{-1} at 1/9 ML coverage) and with spectroscopic studies of vinyl iodide decomposition (1440 and 1306 cm^{-1}) and an Os₃(C=CH₂) carbonyl cluster compound (1470 and 1331 cm^{-1}).⁹

Another possible derivative species is C–CH, which can be formed by C–H cleavage. The ν_{CC} for the most stable di- σ/π -bonded C–CH species ($\mu_3-\eta^2$ configuration), however, is estimated at 1552 cm^{-1} (Table 1). Since this value is much higher than the observed experimental peak of 1417 cm^{-1} , the formation of C–CH can be ruled out.

The differences in the reactivity of regular and deuterated acetylene on the Pt_3Sn surface at 200 K (Figure 2), where a fraction of CH–CH converts to C–CH₂ while CD–CD remains adsorbed molecularly, is likely due to a kinetic isotope effect. Reactions where the rate-limiting step involves an H atom are known to be hindered when the reacting H atom is replaced by the heavier D atom.

The assignment of the peak at 1417 cm^{-1} in the spectrum for C_2H_2 on the Pt_3Sn surface at 200 K to ν_{CC} for C–CH₂ species (Figure 2a) is further supported by the thermal evolution of this spectrum. At 300 K, the intensity of the peak at 1417 cm^{-1} surface decreases, and a new C–C stretching peak appears at 1135 cm^{-1} , which is consistent with ν_{CC} of ethylidyne C–CH₃ species with a reported¹⁰ wavenumber on Pt(111) surfaces of 1118–1124 cm^{-1} . The intensity of this ethylidyne C–CH₃ peak gradually increases upon heating, and at 400 K, an additional peak at 1350 cm^{-1} is observed, which is in agreement with δ_{s-CH_3} (symmetric bending) of C–CH₃ on Pt(111).¹⁰ The formation of ethylidyne C–CH₃ species is consistent with reported acetylene disproportionation on Pt surfaces with the concurrent formation of C–CH and hydrogenation of C–CH₂ species.^{8b,11}

In contrast to the Pt–Sn alloy surfaces, acetylene does not desorb molecularly from the Pt(111) surface, and only decomposition products are detected in TPD measurements. Accordingly, no peaks due to molecular acetylene are observed in the HREELS spectra for both C_2H_2 and C_2D_2 on Pt(111) at 300 K. This is in agreement with our previous studies, which show that acetylene on Pt(111) is adsorbed so strongly that it does not desorb upon heating and, instead, produces surface carbonaceous species by dehydrogenation.¹²

Our new results demonstrate that the presence of Sn not only suppresses acetylene decomposition and intramolecular rearrangement and, as a result, maintains adsorbed acetylene in the molecular form but also eliminates the strongly adsorbed di- σ/π acetylene species, which dominate on pure Pt surfaces.^{6,7,8a} The DFT calculated desorption energy for di- σ/π -bonded acetylene on Pt(111) of 201 kJ/mol (Figure 3a) is in good agreement with the experimental value of ~ 210 kJ/mol reported¹³ based on calorimetric measurements. Calculations with the alloys suggest that di- σ -bonded acetylene on the Pt_3Sn surface (Figure 3b) is less stable than the di- σ/π -bonded species on Pt(111) (Figure 3a) by 50 kJ/mol. Increasing the Sn concentration further reduces the stability of di- σ -bonded acetylene (Figure 3c) by an additional 15 kJ/mol.

A comparison of the main desorption peaks for C_6D_6 evolution (84 amu) in TPD measurements for adsorbed

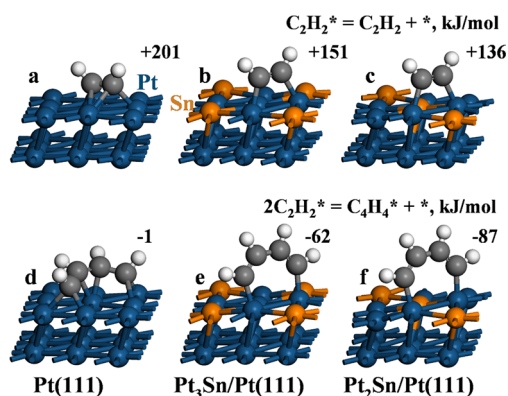


Figure 3. DFT models of adsorbed acetylene and C_4H_4 dimer species. Only two top surface layers are shown for clarity. Models are shown with reaction energies for acetylene desorption and dimerization.

acetylene and benzene on the Pt–Sn surfaces provides strong evidence that the kinetics of benzene formation from acetylene are limited by surface reactions (formation of C_4 or C_6 surface species) and not by benzene desorption. When benzene was adsorbed on the Pt_2Sn surface, the main TPD peak was observed at 320 K. However, when deuterated acetylene was adsorbed, benzene evolution was detected at higher temperatures: 368 K on the Pt_3Sn surface and 375 K on the Pt_2Sn surface, indicating that reaction steps in benzene formation require higher temperatures than benzene desorption and also that once benzene is formed by trimerization, it immediately desorbs from the surface. Moreover, since in contrast to the Pt–Sn surfaces, formation of C_4 species has never been detected on pure Pt surfaces in our new experiments or previous studies,^{2,12} it is likely that the first step of acetylene dimerization to C_4H_4 species is hindered on pure Pt and, as a result, prevents benzene formation.

Our DFT results suggest that the preferential adsorption mode of C_4H_4 species, similarly to that of acetylene, changes in the presence of Sn. While C_4H_4 species are predicted to be multiply bonded to Pt sites ($\mu_5-\eta^4$ configuration in Figure 3d) on the Pt(111) surface, its preferential adsorption mode changes to a metallacycle on a bridge Pt–Pt site on the Pt–Sn surfaces ($\mu_2-\eta^2$ configuration in Figures 3e, f). Importantly, however, due to the presence of strongly adsorbed di- σ/π -bonded acetylene on the Pt(111) surface, the estimated reaction energy for the formation of the surface C_4H_4 species is close to zero (thermoneutral). In contrast, our calculations suggest that C_4H_4 formation becomes exothermic and, therefore, more thermodynamically favorable in the absence of strongly adsorbed di- σ/π -bonded acetylene on the Pt–Sn surfaces. Moreover, the reaction energy is estimated to further decrease noticeably and, thus, to make C_4H_4 formation more preferable with increasing Sn concentration: from -62 kJ/mol on the Pt_3Sn surface to -87 kJ/mol on the Pt_2Sn surface (Figures 3d–f and Table 2).

The effect of Sn alloying on the energetics of acetylene reactions is compared in Table 2. The H transfer reaction with the formation of C– CH_2 surface species is estimated to remain slightly exothermic at the lower Sn concentration on the Pt_3Sn surface and then become slightly endothermic at the higher Sn concentration on the Pt_2Sn surface. The energetics of C–H bond splitting with the formation of C–CH and H surface species are practically unaffected by the presence of Sn. These reaction energies show that the products of acetylene

Table 2. DFT Calculated Reaction Energies for Acetylene Adsorbed on Different Surfaces, kJ/mol

	Pt(111)	Pt_3Sn	Pt_2Sn
desorption	+201	+151	+136
C– CH_2 formation	–19	–19	+13
C–CH + H formation	+101	+95	+100
C_4H_4 formation	–1	–62	–87

rearrangement (C– CH_2) and decomposition (C–CH + H) are destabilized in the presence of Sn to a similar extent as the destabilization of the initial adsorbed acetylene. As a result, the energies of the corresponding reactions are not significantly affected by the presence of Sn or changes in Sn concentration. In contrast, C_4H_4 surface species, which are the product of an associative reaction (dimerization), are destabilized less than adsorbed acetylene in the presence of Sn, and the stability of C_4H_4 surface species relative to adsorbed acetylene increases with increasing Sn concentration. Therefore, elimination of the strongly bonded acetylene in the presence of Sn and the ability to further destabilize surface acetylene by increasing Sn concentration allows control of catalytic selectivity by suppressing rearrangement and decomposition reactions and enhancing associative reactions with the formation of dimers (C_4H_4) and trimers (benzene). The concentration of Sn, however, has to be at an optimal level for balancing catalytic activity and selectivity since our results demonstrate that all hydrocarbon species bind only to Pt surface sites. Consequently, at higher Sn concentrations, the catalytic activity is expected to decline as a result of a decrease in the density of available Pt surface active sites.

This molecular-level understanding of selectivity control and catalytic performance optimization is crucial for optimization of process conditions and development of improved catalyst formulations. As an example, new methods have recently been reported for synthesizing Pt–Sn materials with shape- and composition-controlled (including core–shell) nanoparticles with well-defined Pt and Sn surface sites.¹⁴

In conclusion, adsorption modes of acetylene on Pt–Sn surface alloys were identified by combining vibrational spectroscopic and activity measurements with DFT calculations. Acetylene adsorption modes and reactions on Pt catalytic surfaces can be controlled with Sn alloying. In contrast to pure Pt surfaces where acetylene only decomposes, the presence of Sn opens a new catalytic pathway for associative reactions with the formation of C_4 hydrocarbons and benzene. This new catalytic pathway is linked to changes in acetylene adsorption. The presence of Sn is shown to suppress acetylene decomposition and, as a result, to maintain adsorbed acetylene in the molecular form as weakly adsorbed π - and di- σ -bonded species. The destabilization of adsorbed acetylene makes associative reactions progressively more energetically favorable with increasing Sn concentration. The concentration of Sn, however, needs to be an optimal level for catalytic activity since all hydrocarbon species bind preferentially only to Pt sites.

■ ASSOCIATED CONTENT

Supporting Information

Experimental methods and computational details. This material is available free of charge via the Internet at <http://pubs.acs.org>.

AUTHOR INFORMATION

Corresponding Author

*E-mails: (B.E.K.) BKoel@Princeton.edu, (S.G.P.) Simon.Podkolzin@Stevens.edu.

Present Addresses

[§]Huntsman Advanced Technology Center, 8600 Gosling Road, The Woodlands, Texas 77381 USA.

^{§§}Chemistry Department, Brookhaven National Laboratory, Upton, New York 11973 USA.

Notes

The authors declare no competing financial interest.

ACKNOWLEDGMENTS

The work by Bruce Koel at Princeton University was supported in part by the National Science Foundation under Grant CHE-1129417. Funding for Simon Podkolzin's research was provided by Stevens Institute of Technology. We thank Tao Chen and Yiteng Zheng at Stevens Institute of Technology for help in manuscript preparation. We thank Dr. George B. Fitzgerald at Accelrys Software, Inc. in San Diego, California, USA for help in selecting computational parameters.

REFERENCES

- (1) (a) Cortright, R. D.; Davda, R. R.; Dumesic, J. A. *Nature* **2002**, *418*, 964. (b) Huber, G. W.; Cortright, R. D.; Dumesic, J. A. *Angew. Chem., Int. Ed.* **2004**, *43*, 1549. (c) Huber, G. W.; Shabaker, J. W.; Dumesic, J. A. *Science* **2003**, *300*, 2075. (d) Soares, R. R.; Simonetti, D. A.; Dumesic, J. A. *Angew. Chem., Int. Ed.* **2006**, *45*, 3982.
- (2) Xu, C.; Peck, J. W.; Koel, B. E. *J. Am. Chem. Soc.* **1993**, *115*, 751.
- (3) Szanyi, J.; Paffett, M. T. *J. Am. Chem. Soc.* **1995**, *117*, 1034.
- (4) Overbury, S. H.; Mullins, D. R.; Paffett, M. T.; Koel, B. E. *Surf. Sci.* **1991**, *254*, 45.
- (5) (a) Kim, J.; Fu, J.; Podkolzin, S. G.; Koel, B. E. *J. Phys. Chem. C* **2010**, *114*, 17238. (b) Kim, J.; Welch, L. A.; Olivas, A.; Podkolzin, S. G.; Koel, B. E. *Langmuir* **2010**, *26*, 16401.
- (6) Podkolzin, S. G.; Alcalá, R.; Dumesic, J. A. *J. Mol. Catal. A: Chem.* **2004**, *218*, 217.
- (7) (a) Ibach, H.; Lehwald, S. *J. Vac. Sci. Technol.* **1978**, *15*, 407. (b) Avery, N. R. *Langmuir* **1988**, *4*, 445.
- (8) (a) Okada, T.; Kim, Y.; Trenary, M.; Kawai, M. *J. Phys. Chem. C* **2012**, *116*, 18372. (b) Deng, R.; Jones, J.; Trenary, M. *J. Phys. Chem. C* **2007**, *111*, 1459.
- (9) (a) Zhao, Z. J.; Moskaleva, L. V.; Aleksandrov, H. A.; Basaran, D.; Rösch, N. *J. Phys. Chem. C* **2010**, *114*, 12190. (b) Zaera, F.; Bernstein, N. *J. Am. Chem. Soc.* **1994**, *116*, 4881. (c) Evans, J.; McNulty, G. S. *J. Chem. Soc., Dalton Trans.* **1983**, *4*, 639.
- (10) (a) Deng, R.; Hecceg, E.; Trenary, M. *J. Am. Chem. Soc.* **2005**, *127*, 17628. (b) Malik, I. J.; Brubaker, M. E.; Mohsin, S. B.; Trenary, M. *J. Chem. Phys.* **1987**, *87*, 5544. (c) Chesters, M. A.; McCash, E. M. *Surf. Sci.* **1987**, *187*, L639.
- (11) Cremer, P. S.; Su, X.; Ron Shen, Y.; Somorjai, G. A. *J. Phys. Chem. B* **1997**, *101*, 6474.
- (12) Panja, C.; Saliba, N. A.; Koel, B. E. *Catal. Lett.* **2000**, *68*, 175.
- (13) Kose, R.; Brown, W. A.; King, D. A. *J. Am. Chem. Soc.* **1999**, *121*, 4845.
- (14) Wang, X.; Altmann, L.; Stöver, J.; Zielasek, V.; Bäumer, M.; Al-Shamery, K.; Borchert, H.; Parisi, J.; Kolny-Olesiak, J. *Chem. Mater.* **2013**, *25*, 1400.